Physical basis for wideband resonant reflectors

Robert Magnusson and Mehrdad Shokooh-Saremi

Department of Electrical and Computer Engineering, University of Connecticut, Storrs, CT 06269-2157, USA
robert.magnusson@uconn.edu and saremi@engr.uconn.edu

Abstract: In this paper, we address resonant leaky-mode reflectors made with a periodic silicon layer on an insulating substrate. Our objective is to explain the physical basis for their operation and to quantify the bandwidth provided by a single resonant layer by illustrative examples for both TE and TM polarized incident light. We find that the number of participating leaky modes and their excitation conditions affect the bandwidth. We show that recently reported experimental [1, 2] wideband reflectors operate under leaky-mode resonance. These compact reflectors are new elements with many potential applications in photonic systems. The results presented explaining their physical basis will aid in their continued development.

OCIS codes: (050.1950) Diffraction gratings; (050.6624) Subwavelength structures; (999.9999) Leaky modes; (130.2790) Guided waves; (120.2440) Filters; (999.9999) Reflectors.

References and links

1. C. F. R. Mateus, M. C. Y. Huang, L. Chen, C. J. Chang-Hasnain, and Y. Suzuki, "Broad-band mirror (1.12–1.62 μm) using a subwavelength grating," IEEE Photon. Technol. Lett. **16**, 1676-1678 (2004).
2. M. C. Y Huang, Y. Zhou, and C. J. Chang-Hasnain, "A surface-emitting laser incorporating a high-index-contrast subwavelength grating," Nature Photonics **1**, 119-122 (2007).
3. P. Vincent and M. Neviere, "Corrugated dielectric waveguides: A numerical study of the second-order stop bands," Appl. Phys. **20**, 345-351 (1979).
4. L. Mashev and E. Popov, "Zero order anomaly of dielectric coated gratings," Opt. Comm. **55**, 377-380 (1985).
5. E. Popov, L. Mashev, and D. Maystre, "Theoretical study of anomalies of coated dielectric gratings," Opt. Acta **33**, 607–619 (1986).
6. G. A. Golubenko, A. S. Svakhin, V. A. Sychugov, and A. V. Tishchenko, "Total reflection of light from a corrugated surface of a dielectric waveguide," Sov. J. Quantum Electron. **15**, 886-887 (1985).
7. I. A. Avrutsky and V. A. Sychugov, "Reflection of a beam of finite size from a corrugated waveguide," J. Mod. Opt. **36**, 1527-1539 (1989).
8. R. Magnusson and S. S. Wang, "New principle for optical filters," Appl. Phys. Lett. **61,** 1022-1024 (1992).
9. S. S. Wang and R. Magnusson, "Theory and applications of guided-mode resonance filters," Appl. Opt. **32,** 2606-2613 (1993).
10. Y. Ding and R. Magnusson, "Resonant leaky-mode spectral-band engineering and device applications," Opt. Express **12**, 5661-5674 (2004).
11. H. A. Macleod, *Thin-Film Optical Filters*, (McGraw-Hill, New York, 1989).
12. A. E. Willner, "All mirrors are not created equal," Nature Photonics **1**, 87-88 (2007).
13. A. Yariv and P. Yeh., *Photonics: Optical Electronics in Modern Communications*, 6th ed. (Oxford University Press, New York, 2007).
14. A. Hardy, D. F. Welch, and W. Streifer, "Analysis of second-order gratings," IEEE J. Quantum Electron. **25**, 2096-2105 (1989).
15. Y. Ding and R. Magnusson, "Band gaps and leaky-wave effects in resonant photonic-crystal waveguides," Opt. Express **15**, 680-694 (2007).
16. D. Rosenblatt, A. Sharon, and A. A. Friesem, "Resonant grating waveguide structures," IEEE J. Quantum Electron. **33**, 2038-2059 (1997).
17. R. F. Kazarinov and C. H. Henry, "Second-order distributed feedback lasers with mode selection provided by first-order radiation loss," IEEE J. Quantum Electron. **21**, 144-150 (1985).
18. T. K. Gaylord and M. G. Moharam, "Analysis and applications of optical diffraction by gratings," Proc. IEEE **73**, 894-937 (1985).
19. M. G. Moharam, D. A. Pommet, E. B. Grann, and T. K. Gaylord, "Stable implementation of the rigorous coupled-wave analysis for surface-relief gratings: Enhanced transmittance matrix approach," J. Opt. Soc. Am. A **12**, 1077-1086 (1995).

#90663 - $15.00 USD Received 10 Dec 2007; revised 23 Feb 2008; accepted 24 Feb 2008; published 29 Feb 2008

20. S. T. Peng, T. Tamir, and H. L. Bertoni, "Theory of periodic dielectric waveguides," IEEE Trans. Microwave Theory Tech. **23**, 123-133 (1975).
21. R. Eberhart and J. Kennedy, "Particle swarm optimization," in *Proceedings of IEEE Conference on Neural Networks* (IEEE, 1995) 1942-1948.
22. M. Shokooh-Saremi and R. Magnusson, "Particle swarm optimization and its application to the design of diffraction grating filters," Opt. Lett. **32**, 894-896 (2007).
23. C. F. R. Mateus, M. C. Y. Huang, Y. Deng, A. R. Neureuther, and C. J. Chang-Hasnain, "Ultrabroadband mirror using low-index cladding subwavelength grating," IEEE Photon. Technol. Lett. **16**, 518-520 (2004).

1. Introduction

Subwavelength periodic layers exhibit strong resonance effects that originate in quasi-guided, or leaky, waveguide modes [3-9]. These compact elements yield versatile photonic spectra and surface-localized energy states with controllable Q factors. Using powerful electromagnetic design methods, the spectral bands of these subwavelength resonant leaky-mode elements can be engineered to achieve photonic devices with practical attributes. For example, we have shown that a single periodic layer with one-dimensional periodicity enables narrow-line filters, polarizers, reflectors, and polarization-independent elements [10]. Potential applications include bandpass and bandstop filters, laser mirrors, ultrasensitive biosensors, absorption enhancement in solar cells, security devices, tunable filters, nanoelectromechanical display pixels, and others.

Multilayer thin films are widely applied to implement filters, polarizers, and reflectors for incorporation in various common optical systems [11]. These devices typically consist of stacks of homogeneous layers deposited with precise thicknesses and tight control of index of refraction and absorption. In many cases, a large number of layers, perhaps ~10-100, may be needed to create the spectral and angular attributes required for a particular application. These optical devices operate on the basis of multiple reflections between the interfaces incorporated in a layer stack. In particular, periodic quarter-wave layer systems provide classical high reflectors for bulk laser cavities as well as integrated distributed Bragg reflectors for vertical cavity lasers. Bragg reflectors yield efficient reflection across wide spectral bands [12, 13]. The spectral expressions generated by resonant leaky-mode layers, in some ways, resemble spectral expressions associated with thin-film systems. In other ways, the resonance response is unique and not realizable with homogeneous thin films. Therefore, the functionality and applicability of thin films in optics and photonics technology can be complemented and enhanced by imbuing them with appropriate periodic modulation to achieve leaky-mode resonance.

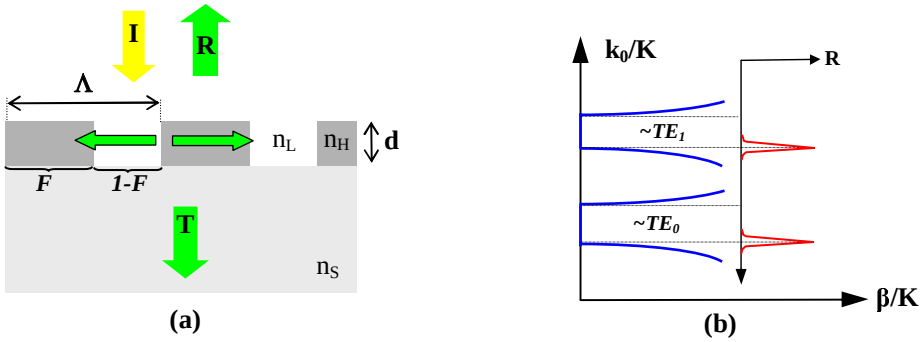

Fig. 1. (a) A schematic view of a subwavelength guided-mode resonance element under normal incidence. A single silicon layer with thickness d, fill factor F, and a two-part period Λ is treated. When phase matching occurs between evanescent diffraction orders and a waveguide mode, a reflection resonance takes place. I, R, and T denote the incident wave, reflectance, and transmittance, respectively. (b) Schematic dispersion diagram of a GMR device at the second stop band. For the symmetric grating profile, a resonance appears at one edge. This picture applies to both TE (electric field vector normal to the plane of incidence) and TM (magnetic field vector normal to the plane of incidence) polarization states. $K = 2\pi/\Lambda$, $k_0 = 2\pi/\lambda$, and β is the propagation constant of a leaky mode.

#90663 - $15.00 USD Received 10 Dec 2007; revised 23 Feb 2008; accepted 24 Feb 2008; published 29 Feb 2008

Figure 1(a) shows the model device to be treated. It is a subwavelength reflector consisting of a modulated silicon layer ($n_H = n_{Si} = 3.48$) on a SiO_2 substrate ($n_S = n_{SiO2} = 1.48$). It is necessary that the structure form a waveguide grating such that the periodic layer (Si) possesses higher refractive index than the adjacent regions (air, silica). The reflector works under a guided-mode resonance (GMR), which arises when the incident wave couples to a leaky waveguide mode by phase matching with the second-order grating [14, 15]. Under normal incidence, counter-propagating leaky modes form a standing wave in the grating as indicated in Fig. 1(a). As the modes interact with the waveguide grating, they reradiate reflectively [16]. A schematic dispersion diagram is shown in Fig. 1(b). The device works in the second stop band corresponding to the second-order grating [15]. A given evanescent diffraction order can excite not just one but several leaky modes. Thus, in Fig. 1(b), we show the stop bands for the first two TE modes to emphasize this point. At each stop band, a resonance is generated as denoted in Fig. 1(b) also. The fields radiated by these leaky modes in a grating with a symmetric profile can be in phase or out of phase at the edges of the band [17, 3]. At one edge, there is a zero phase difference and hence the radiation is enhanced while at the other edge, there is a π phase difference inhibiting the radiation. In this case, if $\beta = \beta_R + j\beta_I$ is the complex propagation constant of the leaky mode, $\beta_I = 0$ at one edge, implying that no leakage is possible at that edge. In this paper, for clarity, we treat resonance elements with two-part periods which can only have symmetric profiles.

2. Numerical methods and assumptions

We limit the study to single-layer structures modulated with one-dimensional (1D) binary profiles. For simplicity and numerical expediency, it is assumed that the gratings are transversely infinite and that the materials are lossless and dispersion free. The spectral analysis of these structures is performed using rigorous coupled-wave analysis (RCWA) for both TE and TM polarizations. This method models exactly electromagnetic wave interactions with periodic layered structures, rigorously satisfying the electromagnetic boundary conditions for each polarization, and expeditiously providing associated reflection and transmission diffraction efficiencies [18, 19]. Modal methods are utilized to compute field profiles, patterns, and propagating-wave diffraction efficiencies for both polarization states [20]. The spectra computed with the modal and RCWA techniques are in excellent agreement. Approximate modal curves are determined by solving the eigenvalue equation associated with slab dielectric waveguides [9]. An inverse numerical technique, particle swarm optimization (PSO) [21], is utilized to design the broadband reflectors presented. The period, thickness, and fill factor of the grating layer are the design parameters. A root-mean-square fitness function is chosen to ensure the numerical quality of the solutions [22].

3. Results

As design target for the first example, we aim for reflectance $R_0 = 1.0$ over the 1.45-2.0 μm wavelength band in TM polarization. The parameters that are optimized to achieve the target reflectance are period, thickness, and fill factor. Figure 2(a) shows the reflectance and transmittance of the designed element in which $\Lambda = 0.766$ μm, $d = 0.490$ μm, $F = 0.7264$, $n_H = 3.48$, $n_L = 1.0$, and $n_S = 1.48$. The spectrum for which $R_0 > 0.99$ exhibits a bandwidth of ~520 nm. There are three transmittance dips inside the high-reflectance band, each of which corresponding to a guided-mode resonance at which the transmittance approaches zero. Thus, this high-reflection band is supported by a blend of three leaky modes. Figure 2(b) illustrates the amplitudes of the magnetic modal fields inside the grating structure and in the surrounding media at the center resonance which arises at 1.620 μm. The amplitude of the incident zero-order wave is denoted by S_0 whereas the first evanescent wave has amplitude S_1. This low-Q resonance raises the internal field strength of the first-order leaky mode by ~×3 relative to the excitation field. The S_1 field shows a predominant TM_0 shape that nevertheless also exhibits TM_2 features with two nulls in the low-amplitude region near the input edge. There is an appreciable second-order field (S_2) in the structure as seen in the figure. It is important to note that the zero-order field fits well into the layer which is ~one wavelength in thickness at

#90663 - $15.00 USD Received 10 Dec 2007; revised 23 Feb 2008; accepted 24 Feb 2008; published 29 Feb 2008

resonance (compare d = 0.490 μm and λ/N = 1.620/3.0 = 0.540 μm using the second-order effective-medium-theory refractive index of the grating layer N = 3.0). This sets up an efficient excitation of the leaky modes; i.e. the input wave "pumps" the structure well, a key condition in achieving broad reflectance spectra.

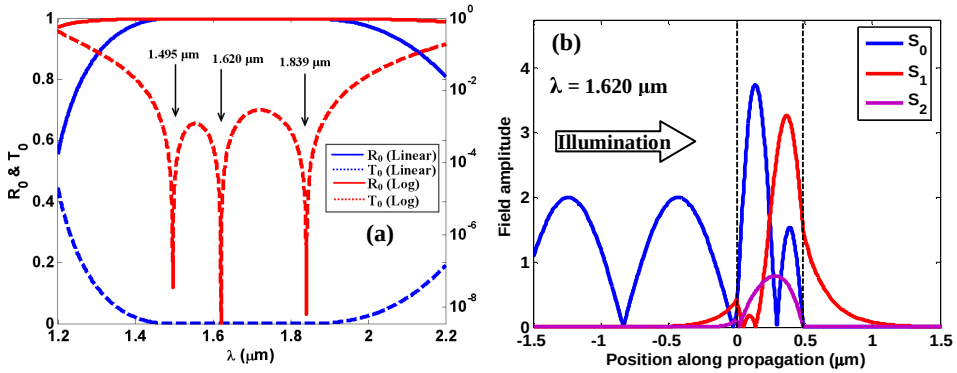

Fig. 2. (a) Zero-order reflectance and transmittance spectra of an example broadband reflector operating in TM polarization. The $R_0 > 0.99$ bandwidth is ~520 nm. For clarity, the spectra are plotted on both linear and logarithmic scales. (b) Amplitudes of the magnetic modal fields inside the grating layer and in the surrounding media at the wavelength of the center resonance.

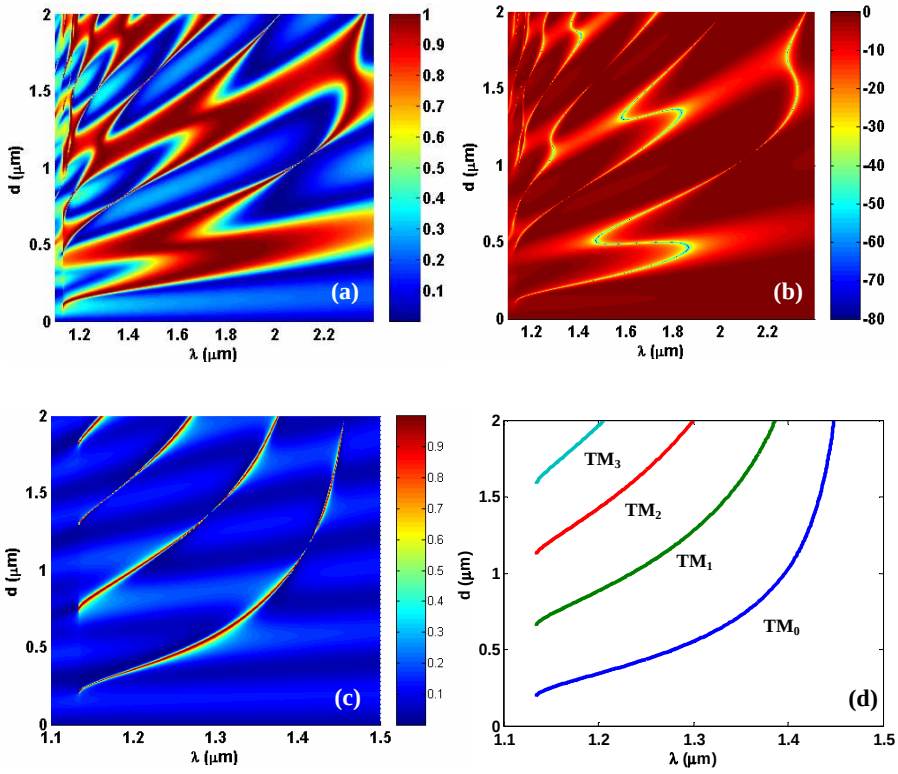

Fig. 3. (a) Reflectance map R(λ,d) pertaining to the broadband reflector and the results in Fig. 2. (b) Transmittance map T(λ,d) in dB. (c) Reflectance map R(λ,d) for a resonance layer with reduced contrast (n_H = 2.0 and n_L = 1.3417). (d) Modal curves for the first four modes excited by the first evanescent diffraction order setting n_{film} = 1.92.

#90663 - $15.00 USD Received 10 Dec 2007; revised 23 Feb 2008; accepted 24 Feb 2008; published 29 Feb 2008

Figure 3(a) displays a color-coded reflectance map R(λ,d) drawn versus wavelength and grating thickness for the same example. Numerous S-shaped high reflection regions appear showing the evolution of the reflectance from narrow to broad resonance bands. Figure 3(b) illustrates the associated transmittance versus wavelength and thickness in dB, clearly revealing the sharp resonance loci. Note the flat-band locus near d = 0.5 μm which corresponds to the results in Fig. 2.

To further emphasize the leaky-mode resonance origin of the wideband reflectance spectra, we connect the behavior of this modulated waveguide to its homogeneous counterpart. The modal character of the device is revealed upon reduction of the refractive-index modulation while keeping the average refractive index of the waveguide layer fixed. Taking n_H = 2.0 and n_{ave} = 1.7314 (zero-order effective medium value), n_L is calculated to be 1.3417. Figure 3(c) shows the R(λ,d) map for this weakly modulated structure. Note that a broad reflection region is beginning to form between the two lowest modes at thickness d ~ 0.8 μm. Sequential calculations performed while gradually increasing the modulation show that the map in Fig. 3(c) morphs into that in Fig. 3(a) for full modulation. Finally, modal curves are obtained by solving the eigenvalue equation of the equivalent homogenous slab waveguide [9]. The results are given in Fig. 3(d) for the first four modes setting n_{film} = 1.92 which is in reasonable agreement with the second-order effective index of the grating layer which is 1.82. There is unmistakable qualitative agreement between these two graphs.

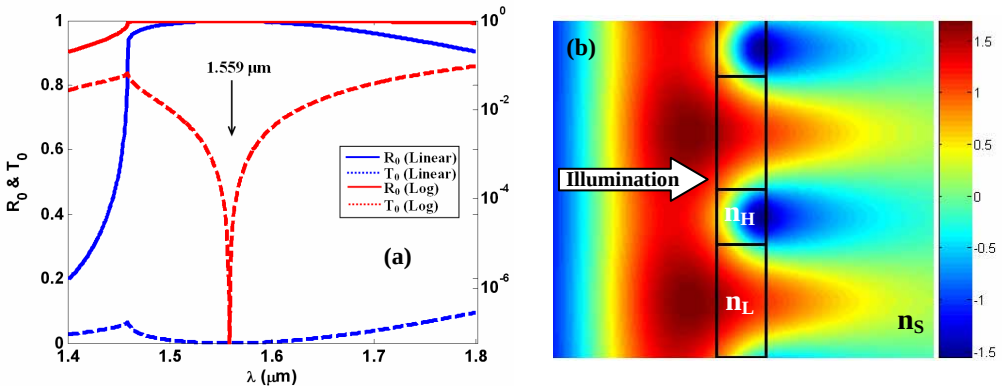

Fig. 4. (a) TE polarized spectra for a simple single-layer reflector. The bandwidth is ~125 nm for reflectance R_0 > 0.99. (b) Electric field distribution pattern at the resonance wavelength of 1.559 μm.

Wideband resonance reflectors are not limited to the TM polarization state. Figure 4(a) provides computed reflectance and transmittance spectra for TE polarization. For this design, Λ = 0.986 μm, d = 0.228 μm, and F = 0.329. The spectral width is ~125 nm for a flat band with R_0 > 0.99. Figure 4(b) displays the electric field distribution pattern at the resonance wavelength. A dominant TE_0 leaky mode is generated by the first evanescent diffraction order. Moreover, by dividing the period into four parts ({Si, air, Si, air} with corresponding fill factors {F_1, F_2, F_3, F_4; $F_1+F_2+F_3+F_4$ = 1.0}), very broad reflection bandwidths with R_0 > 0.99 are realizable; these may exceed ~600 nm in both TE and TM polarization for a single Si layer without substrate enhancement [10]. In essence, the four-part period imbues the periodic layer with a rich set of Fourier harmonics with concomitant emergence of additional spectral features not available for the two-part case in Fig. 1(a).

Mateus et al. reported an experimental wideband reflector operating around the 1.55 μm wavelength [1]. The element consists of a silicon grating over a silica sublayer (with thickness d_L) on a silicon substrate. In a prior paper focusing on reflector design [23], they provided a set of optimized parameters as Λ = 0.7 μm, d = 0.46 μm, d_L = 0.83 μm, and F = 0.75. We use

#90663 - $15.00 USD Received 10 Dec 2007; revised 23 Feb 2008; accepted 24 Feb 2008; published 29 Feb 2008

this set in Fig. 5(a) which shows the spectra of this reflector including a sharp leaky-mode transmission minimum consistent with the results presented above. The computed reflection bandwidth is ~467 nm for $R_0 > 0.99$ with TM polarization. Figure 5(b) shows the effect of the sublayer/substrate combination on the reflectance spectrum. Without the sublayer, the bandwidth for this design is ~385 nm. Therefore, in this case, the sublayer extends the flat band by ~80 nm or ~20%.

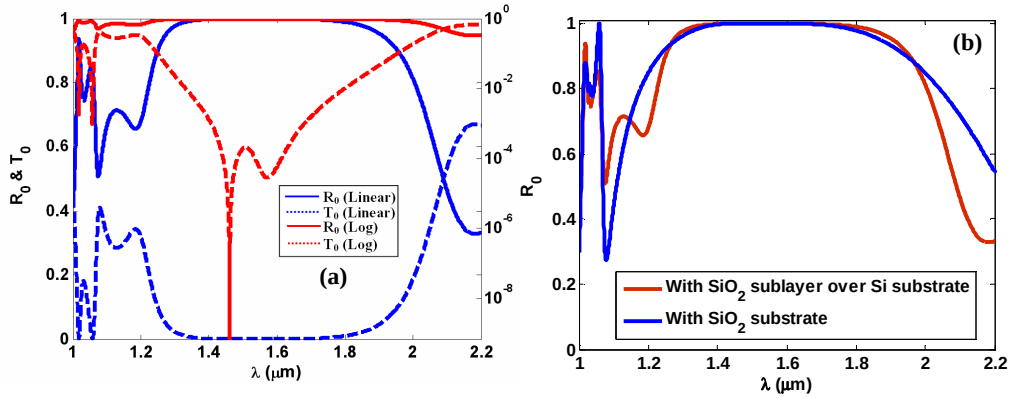

Fig. 5. (a) Spectra of a broadband reflector with $\Lambda = 0.7$ μm, $d = 0.46$ μm, $d_L = 0.83$ μm, and $F = 0.75$. (b) Computed results showing the effect of the sublayer/substrate combination on the reflectance spectra.

4. Conclusions

In summary, we have explained the physical basis for wideband subwavelength grating reflectors. For clarity, in this paper, we treat the simplest possible resonance element which is a single layer with one-dimensional periodicity and two-part period. Thus, strongly-modulated resonant leaky-mode reflectors made with a periodic silicon layer on an insulating (silica) substrate have been characterized by rigorous numerical analysis. A particular TM polarized reflector is found to provide a 520 nm bandwidth at 99% reflectance. It is shown that this flat band is contributed by three cooperating leaky modes. These modes are efficiently excited ("pumped") by the incident wave as the grating layer thickness is one wavelength (in general, multiple of ~λ/2N) at the center resonance. On reduction of the grating modulation contrast, computed reflectance maps approach the modal plots corresponding to a homogeneous waveguide slab in both location and shape, further supporting the leaky-mode resonance argument. A single-layer TE reflector with 125 nm bandwidth is also provided demonstrating the viability of these elements in both polarization states. Finally, we show that reported TM-polarized experimental [1] wideband reflectors operate under leaky-mode resonance. In fact, a low-Q resonance causes the wideband reflection with the bandwidth being extended by interaction with the silicon substrate.

Leaky-mode resonance devices belong to the class of periodic nanophotonic structures, photonic crystals, and diffractive elements that are of growing importance for applications in active and passive devices such as filters, lasers, displays, and sensors. The results presented explain the physics of their operation as broadband reflectors and may contribute to their further development and utility. Excitation of leaky modes is a necessary, but not sufficient, condition for broadband reflectance. Additionally, the leaky-mode spectra must be shaped by proper choice of the device parameters. As in this work, such optimized parameters can be effectively established using inverse mathematical design methods like PSO. Future research will explore bandwidth enhancements achievable by more complex architectures including sublayer-substrate enhancements, multi-component periods, and additional layers.

#90663 - $15.00 USD Received 10 Dec 2007; revised 23 Feb 2008; accepted 24 Feb 2008; published 29 Feb 2008

Acknowledgements

The authors thank Y. Ding for his contributions in developing parts of the analysis codes. This material is based, in part, upon work supported by the National Science Foundation under Grant No. ECS-0524383.

#90663 - $15.00 USD Received 10 Dec 2007; revised 23 Feb 2008; accepted 24 Feb 2008; published 29 Feb 2008